

# Evolutionary and Genetic Algorithms Applied to Li<sup>+</sup>-C System: Calculations Using Differential Evolution and Particle Swarm Algorithm

N. Chakraborti, R. Jayakanth, S. Das, E. D. Çalişir and Ş. Erkoç

(Submitted September 15, 2005)

A set of empirical potentials based upon two and three body interactions were constructed for the Li<sup>+</sup>-C system and structural optimizations for various assemblages containing Li<sup>+</sup> ions and graphene sheets were conducted using some emerging evolutionary and genetic algorithms, differential evolution, and particle swarm optimization in particular. Some limited molecular dynamics calculations were also performed. The results are discussed and analyzed with reference to the lithium ion batteries, where the graphite-Li<sup>+</sup> assemblages traditionally constitute the negative electrode, for which the present results are highly pertinent.

**Keywords** optimization, *ab initio* methods, binary system, calculations, computation, first principles, modeling, genetic algorithm

## 1. Introduction

Rechargeable lithium ion batteries provide a unique combination of larger capacity, smaller size, and lighter weight along with a moderate price. Such devices are of immense current and potential importance for various utilities like cellular phones, laptop computers, and electric vehicles, and fundamental studies related to their positive and negative electrodes as well as the electrolytes are crucial for augmenting the performance of such batteries in order to sustain their competitiveness in the rapidly emerging global energy market.

The present study dealing with the Li<sup>+</sup>-C system has a direct relevance to the anodic region of the lithium ion batteries. Lithium metal cannot be directly used for this purpose, as dendrites readily form during the electrochemical process leading to some severe short circuits. The usual technique to circumvent this problem is to intercalate lithium ions in the lattice of graphite, from where it can be de-intercalated at a low potential. Although the stoichiometry of the lithium present in the graphite lattice is generally taken as the rather stable configuration of LiC<sub>6</sub>, it remains highly relevant to look into the stabilities of various other

configurations, in order to suggest an alternate. More lithium ions, capable of reversible release that one can accommodate in the lattice would lead to an augmentation of the battery performance. In this study we have systematically investigated the consequence of inserting various amounts of lithium ions in the graphite lattice, and computed both the optimized structural configurations and the corresponding energy. Further details are provided below.

## 2. Developing the Energy Functional

In this work an empirical many-body potential energy functional was developed for the carbon-lithium ion system assuming that the total interaction energy ( $\Phi$ ) of any Li<sup>+</sup> and C assemblage could be taken as the algebraic sum of the total two-body ( $\phi_2$ ) and three-body ( $\phi_3$ ) contributions, so that

$$\Phi = \phi_2 + \phi_3 \quad (\text{Eq 1})$$

We define  $\phi_2$  as the sum of C-C, C-Li<sup>+</sup> and Li<sup>+</sup>-Li<sup>+</sup> interactions, whereas  $\phi_3$  contains only the C-C-C three-body interactions. All carbon interactions (C-C and C-C-C) are represented by Tersoff potentials.<sup>[1,2]</sup> The explicit form of the total two-body and three-body energies for carbon are expressed, respectively, as:

$$\begin{aligned} \phi_2(C-C) &= A \sum_{i<j}^N U_{ij}^{(1)} \\ \phi_3(C-C-C) &= -B \sum_{i<j}^N U_{ij}^{(2)} \left[ 1 + \beta^n \left( \sum_{k \neq i,j}^N W_{ijk} \right)^n \right]^{-1/2n} \end{aligned} \quad (\text{Eq 2})$$

Here  $U_{ij}$  and  $W_{ijk}$ , respectively, denote two- and three-body interactions and are explicitly described as:

N. Chakraborti, R. Jayakanth, and S. Das, Department of Metallurgical & Materials Engineering, Indian Institute of Technology, Kharagpur, WB 721 302, India. Contact e-mail: Nirupam.Chakraborti@iitkgp.ac.in E. D. Çalişir, and Ş. Erkoç, Department of Physics, Middle East Technical University, 06531 Ankara, Turkey.

$$U_{ij}^{(1)} = f_c(r_{ij}) \exp(-\lambda_1 r_{ij}) \quad (\text{Eq 3})$$

$$U_{ij}^{(2)} = f_c(r_{ij}) \exp(-\lambda_2 r_{ij})$$

$$W_{ijk} = f_C(r_{ik})g(\theta_{ijk}) \quad (\text{Eq 4})$$

where

$$g(\theta_{ijk}) = 1 + \frac{c^2}{d^2} - \frac{c^2}{d^2 - (h - \cos \theta_{ijk})^2} \quad (\text{Eq 5})$$

$$f_c(r) = \begin{cases} 1 \\ \frac{1}{2} - \frac{1}{2} \sin \left[ \frac{\pi}{2} (r - R)/D \right] \\ 0 \end{cases}$$

for  $r < R - D$

for  $R - D < r < R + D$  (Eq 6)

for  $r > R + D$

where,  $r_{ij}$  is the distance between atom  $i$  and atom  $j$ ,  $\theta_{ijk}$  is the bond angle between bonds  $ij$  and  $ik$ ,  $R$  and  $D$  are such that the cut-off function  $f_c(r)$ , which has a continuous value and derivative for all  $r$ , goes from 1 to 0 in a small range  $D$  around  $R$ .

The parameters of the Tersoff potential<sup>[2]</sup> for carbon are listed in Table 1.

The interactions between C-Li<sup>+</sup> were expressed by the following pair-potential function:

$$U_{ij} = \frac{A_1}{r_{ij}^{\lambda_1}} \exp(-\alpha_1 r_{ij}^2) - \frac{A_2}{r_{ij}^{\lambda_2}} \exp(-\alpha_2 r_{ij}^2) \quad (\text{Eq 7})$$

The numerical values of the PEF parameters used in Eq 7 are listed in Table 2.

These parameters were determined by least-square fitting the pair-function to the interaction energy data points obtained by density functional theory (DFT) method<sup>[3]</sup> calculations realized for C-Li<sup>+</sup> diatomic molecule in its ground state. B3LYP exchange-correlation functional<sup>[4,5]</sup> along with 3-21G basis set<sup>[6]</sup> was used. DFT calculations were performed by Gaussian-98 package program.<sup>[7]</sup> Gaussian calculations however, were not attempted for the lowest-energy configurations, as the

computing facility currently at our disposal would be inadequate for that. Since the Gaussian calculations are not the major objective of this study, their detailed discussions are not included in this article.

The interactions between Li<sup>+</sup>-Li<sup>+</sup> were taken as purely repulsive, since Li<sup>+</sup> ion is a closed shell atom, any bonding formation would be highly improbable:

$$U_{ij} = \frac{a'}{r_{ij}} \exp(-b' r_{ij}) \quad (\text{Eq 8})$$

The parameters  $a'$  and  $b'$  used in Eq 8 were predicted from quantum chemical calculations. The parameter set used in the present study is listed in Table 3.

In summary, Tersoff potential parameters were obtained from the literature,<sup>[1,2]</sup> and both, C-Li<sup>+</sup> and Li<sup>+</sup>-Li<sup>+</sup> pair-potentials were calculated using the Gaussian procedure, where several single point calculations were performed, and the relevant parameters were determined by fitting the results to their corresponding equations. Both attractive and repulsive terms were used to construct the Tersoff and the C-Li<sup>+</sup> pair potentials; the Li<sup>+</sup>-Li<sup>+</sup> pair-potential however, was taken as purely repulsive.

To check the validity of the potentials obtained through this procedure, the results were compared against the quantum calculations for the C-Li<sup>+</sup> dimer, and virtually identical values were obtained when the potential function was fitted to the quantum results.

### 3. The Evolutionary Optimization Algorithms

Once the potentials are known, the next task is to optimize the geometry of various Li<sup>+</sup>-C assemblages, considering a graphite type of configuration for the carbon atoms. This leads to a minimization of the energy functional, and for such problems, in recent times, biologically inspired genetic and evolutionary algorithms<sup>[8-11]</sup> are being very efficiently used in a host of studies.<sup>[12-21]</sup> In this investigation we have used two different types of evolutionary algorithms, Differential Evolu-

**Table 3 The parameters for lithium-lithium interaction**

$A'$	$b'$
0.5429457 eV Å	0.0033331 Å <sup>-1</sup>

**Table 1 The parameters for carbon-carbon interaction**

A	B	$\Lambda_1$	$\Lambda_2$	$\beta$	n	c	d	h	R	D
1393.6 eV	346.74 eV	3.4879	2.2119	$1.5724 \times 10^{-7}$	0.72751	38049	4.3484	-0.57058	1.95 Å	0.15 Å

**Table 2 The parameters for carbon-lithium interaction (energy in eV, distance in Å)**

$A_1$	$A_2$	$\alpha_1$	$\alpha_2$	$\Lambda_1$	$\Lambda_2$
38.4637591	21.3476845	0.229357324	0.133259571	1.71241891	1.16453151

## Section I: Basic and Applied Research

tion (DE) and Particle Swarm Optimization (PSO). The basic features of these algorithms are briefly provided below.

### 3.1 Differential Evolution

This is a greedy, real-coded genetic algorithm<sup>[22,23]</sup> noted for its fast convergence properties. We have utilized DE for many of our earlier work<sup>[18,24,25]</sup> where the basic features of this algorithm are discussed at length and therefore are not repeated here. The crossover procedure that we have adopted here is very similar to what has been discussed earlier. However, for any population member  $\mathfrak{S}_i$ , its crossover partner  $\mathfrak{S}_\oplus$  is generated as:

$$\mathfrak{S}_\oplus = \mathfrak{S}_\mathfrak{N} + \gamma_I(\mathfrak{S}_1 - \mathfrak{S}_2) + \gamma_{II}(\mathfrak{S}_3 - \mathfrak{S}_4) \quad (\text{Eq 9})$$

where  $\mathfrak{S}_\mathfrak{N}$  denotes the best solution at the onset of the current generation. The remaining  $\mathfrak{S}$  terms in Eq 9 refer to four randomly picked members of the population, different from  $\mathfrak{S}_i$ . The user-defined parameters  $\gamma_I$  and  $\gamma_{II}$  were taken as 0.1 each and a crossover probability of 0.8 worked satisfactorily for this problem. A population size slightly over  $10 \times$  the number of variables would usually suffice in most calculations.

### 3.2 The Particle Swarm Algorithm

This powerful evolutionary optimizer emulates the group behavior of a certain types of animal species; say for example, a flock of birds or a school of fish.<sup>[26–28]</sup> Like most genetic and evolutionary algorithms, a *population* of possible solutions is considered here, constituting the *swarm* in this algorithm. Here each *individual*, say a bird or a fish, is termed as a *particle*. The idea is that the whole swarm tends to move towards the optimum point in a multi-dimensional solution hyperspace, shown schematically in Fig. 1, where the flagged peak is the ultimate target for the entire swarm. Each particle has got its own velocity vector, consisting of both magnitude and direction different from the rest, and there is obviously a particle that is leading the entire flock in its quest for the flagged peak. The swarm, the way it is constructed in this algorithm, has got a collective memory of such leaders, while every individual

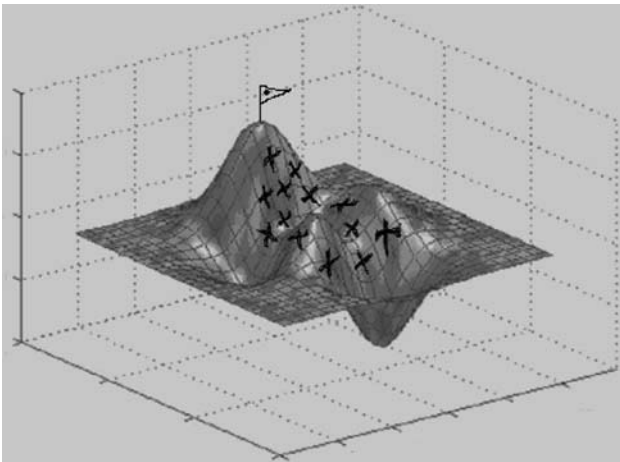


**Fig. 1** Schematics of particle swarm optimization: particles in a hyperspace.

member has got a memory of its own best performance so far. Based upon this information, each particle can alter its own course, following the velocity correction procedure discussed below.

At every *iteration cycle*, analogous to a *generation* in the usual Genetic Algorithms sense, each particle updates its velocity vector based upon the two criteria mentioned before: its own best performance so far and the global best performance that has been encountered in the swarm till now. The level of performance is measured in the same way, as the *fitness* is determined in most Genetic Algorithms. Consequently, for function maximization problems, a higher function value would result in a higher fitness and the converse remains true for the minimization case. At any iteration cycle  $i$ , a particle  $j$  updates its velocity vector  $V_j^i$  as

$$\vec{V}_j^i = \varpi \vec{V}_j^{i-1} + \Gamma_1 \mathfrak{R}_1 (\vec{x}_{j,IBST}^{i-1} - \vec{x}_j^{i-1}) + \Gamma_2 \mathfrak{R}_2 (\vec{x}_{j,GBST}^{i-1} - \vec{x}_j^{i-1}) \quad (\text{Eq 10})$$

where  $\varpi$  denotes the user defined *inertia weight*,  $\vec{x}$  terms denote various position vectors, the subscript *IBST* denotes the individual best position attained by the particle and *GBST* denotes the global best position attained so far by any member of the current swarm, the  $\Gamma$  terms denote user defined constants, usually adjusted through a systematic trial and error, and the  $\mathfrak{R}$  terms are uniform random numbers in the interval  $[0,1]$ .

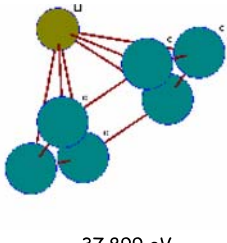
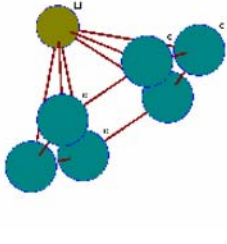
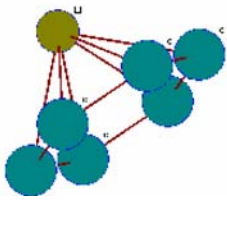
Using the newly constructed velocity vectors, the position vectors are updated as:

$$x_j^i = \vec{x}_j^{i-1} + \vec{V}_j^i \quad (\text{Eq 11})$$

The first term in Eq 10 represents the inertia contribution to the motion of the particles, while the acceleration effects are brought in through the second and the third terms. The readers who perhaps are worried about the dimensional consistencies of Eqs 10 and 11 should note that the dimension of the  $\Gamma \mathfrak{R}$  terms in (Eq 10) could be taken as  $(\text{time})^{-2}$ . This way, the second and the third terms in Eq 10 assume the dimension of acceleration. To get the correct dimension of velocity, as required by the left hand side, one needs to multiply them by  $\Delta t$ , the time step, which becomes unity in the present case, denoting changes from iteration  $i-1$  to  $i$ . Similarly, the second term in Eq 11 assumes the correct dimension when taken as  $\vec{V}_j^i \Delta t$ . However, the present form results through the implicit assumption that  $\Delta t$  equals 1.<sup>1</sup>

Since the particles have the routinely updated collective memory of *GBST*, and the individual memory of *IBST*, repeated applications of the Eqs 10 and 11 become possible, and it drives the swarm very efficiently towards the optimum point. In some versions of PSO, which has not been followed here, the acceleration term also include a contribution from *LBST*, the local best position.<sup>[28]</sup> This denotes the best possible position in the neighborhood of particle  $j$ , and the concept of the neighborhood can be easily implemented in such algorithms, utilizing the idea of *Niche* that widely prevails in the Genetic Algorithms literature.<sup>[9]</sup>

<sup>1</sup>To the readers familiar with Real-coded Genetic Algorithms,<sup>[9]</sup> the whole procedure should appear as a special type of crossover.

Differential Evolution	 -37.899 eV	C1	0.011979	1.394647	-0.002167
		C2	1.245532	0.741335	0.008270
		C3	1.257711	-0.707472	0.011850
		C4	0.026715	-1.425623	-0.023856
		C5	-1.203855	-0.702685	-0.016645
		C6	-1.259136	0.730619	-0.011792
		Li1	-0.071780	0.066546	1.953024
		Particle Swarm Optimization	 -37.613 eV	C1	0.000000
C2	1.230600	0.710500	0.000000		
C3	1.230600	-0.710500	0.000000		
C4	0.000000	-1.421000	0.000000		
C5	-1.230600	-0.710500	0.000000		
C6	-1.230600	0.710500	0.000000		
Li1	-0.010678	0.015912	1.997672		
Molecular-dynamics	 -37.144 eV	C1	-1.21443	0.70095	-0.00979
C2	-1.21387	-0.70093	-0.00890		
C3	-0.00008	-1.40174	-0.00891		
C4	1.21429	-0.70128	-0.00988		
C5	1.21488	0.70130	-0.01093		
C6	-0.00008	1.40273	-0.01088		
Li1	0.02838	0.04587	1.75939		

**Fig. 2** Optimized ground state configuration of  $C_6Li$  computed using various techniques. The Cartesian coordinates for various atoms are indicated on the right.

#### 4. Computational

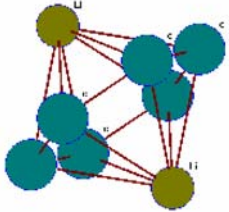
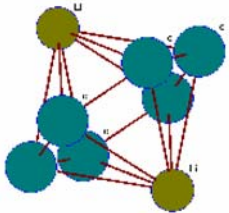
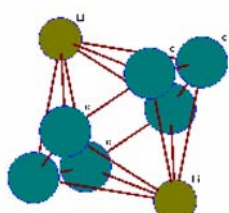
Tailor-made C codes were developed during this study both for Differential Evolution and Particle swarm Optimization, and were executed under a SUSE LINUX environment in an IBM P-series Open Power Server 720 workstation. A limited number of Molecular-dynamics (MD) simulations were also performed for occasional comparison of results. During the MD simulations the equations of motion of the particles<sup>2</sup> were solved by using the Verlet algorithm<sup>[29]</sup> and the canonical ensemble molecular-dynamics NVT<sup>[29]</sup> was employed, where the number of particles  $N$ , the volume  $V$ , and the temperature  $T$  were fixed. The total energy is not a conserved quantity for constant temperature in canonical ensemble. However, the average kinetic energy is a constant due to its coupling with the temperature. The temperature rescaling was taken into account at every MD step and the temperature of the system was kept constant at a given temperature. One time step was taken as

$10^{-16}$  s. The initial velocities of the particles were determined from the Maxwell distribution at the given temperature. The simulations were carried out at low temperature (1K) and 100000 time steps were found to be adequate for relaxation. This low temperature was chosen because Genetic and Evolutionary algorithms do not consider temperature, and the low temperature was used for the sake of comparison under a normalized condition. However, had it been a solely MD based study, annealing from some higher temperature perhaps would be desirable. The time step is a fixed parameter in the molecular dynamics simulations. It remained unaltered.

#### 5. Results and Discussion

Although carbon can exist in many different forms, in this study we have presumed that it exists as the hexagonal graphene sheets, which till now is the prevailing form used in the lithium ion batteries worldwide. Initially we have started with just a single layer of six carbon atoms following the graphite symmetry. Initially a lone  $Li^+$  ion and subsequently a

<sup>2</sup>Here the term *particle* represents an atom. It should not be confused with the particles in PSO.

Differential Evolution	 <p style="text-align: center;">-43.377 eV</p>	C1	0.00000	1.42100	0.00000
		C2	1.23060	0.71050	0.00000
		C3	1.23060	-0.71050	0.00000
		C4	0.00000	-1.42100	0.00000
		C5	-1.23060	-0.71050	0.00000
		C6	-1.23060	0.71050	0.00000
		Li1	-0.00916	0.02772	-1.65647
		Li2	0.07263	0.08899	1.60788
		Particle Swarm Optimization	 <p style="text-align: center;">-44.819 eV</p>	C1	0.00000
C2	1.23060	0.71050		0.00000	
C3	1.23060	-0.71050		0.00000	
C4	0.00000	-1.42100		0.00000	
C5	-1.23060	-0.71050		0.00000	
C6	-1.23060	0.71050		0.00000	
Li1	0.00000	0.00000		-1.42100	
Li2	0.00000	0.00000		1.42100	
Molecular-dynamics	 <p style="text-align: center;">-44.596 eV</p>	C1		-1.20208	0.69406
C2		-1.20208	-0.69401	0.00001	
C3		0.00002	-1.38805	0.00002	
C4		1.20212	-0.69401	0.00002	
C5		1.20213	0.69406	0.00001	
C6		0.00003	1.38810	0.00002	
Li1		0.00004	0.00003	1.87768	
Li2		0.00001	0.00005	-1.87764	

**Fig. 3** Optimized ground state configuration of  $C_6Li_2$  computed using various techniques. The Cartesian coordinates for various atoms are indicated on the right.

couple of them were allowed to interact with this graphite hexagon, resulting in the  $C_6Li$  and  $C_6Li_2$  configurations at the computed ground state. One needs to recall at this stage that in most battery applications the graphite intercalation compound prevailing at the anode is taken as the one having the  $LiC_6$  symmetry,<sup>[30,31]</sup> and the so called super dense configuration of  $LiC_3$  is also possible to obtain through controlled ball milling.<sup>[31]</sup> The second compound is stable at room temperature and normal pressure and its electrical properties make it a strong contender for the negative electrode. We have calculated these two structures using Differential Evolution, Particle Swarm Optimization as well as the Molecular-dynamics techniques. The optimized configurations are of reasonable similarity, as presented in Fig. 2 and 3.

Additional layers of graphite hexagons were now progressively added, and the number of  $Li^+$  was gradually increased up to four, and the energy minimization continued using both Differential Evolution and Particle Swarm Optimization techniques. The series of ground state configurations that resulted in

through these procedures are presented in Fig. 4. It is interesting to note that both the evolutionary techniques have produced better results than the molecular dynamics simulations. It's simply because the evolutionary techniques, through crossover and mutation are able to pass over the energy barriers, an ability which the molecular dynamics method does not have, particularly at low temperatures. This in fact presents a strong justification for using the Genetic Algorithms for such calculations, where the energy contours are highly multi-modal and in the terminology of the evolutionary computing, one encounters a very difficult *fitness landscape*.<sup>[9]</sup>

The results that are shown in Fig. 4 have been obtained without any special restrictions on the location of the  $Li^+$  ions in the lattice. However, in order to disperse the lithium ions widely in the lattice, and to overcome the strong repulsive interaction between the lithium cations, we have recalculated some larger clusters, implementing the constraints listed in Table 4.

The constrained and unconstrained structures are compared in Fig. 5. Particularly for the larger clusters, their atomic



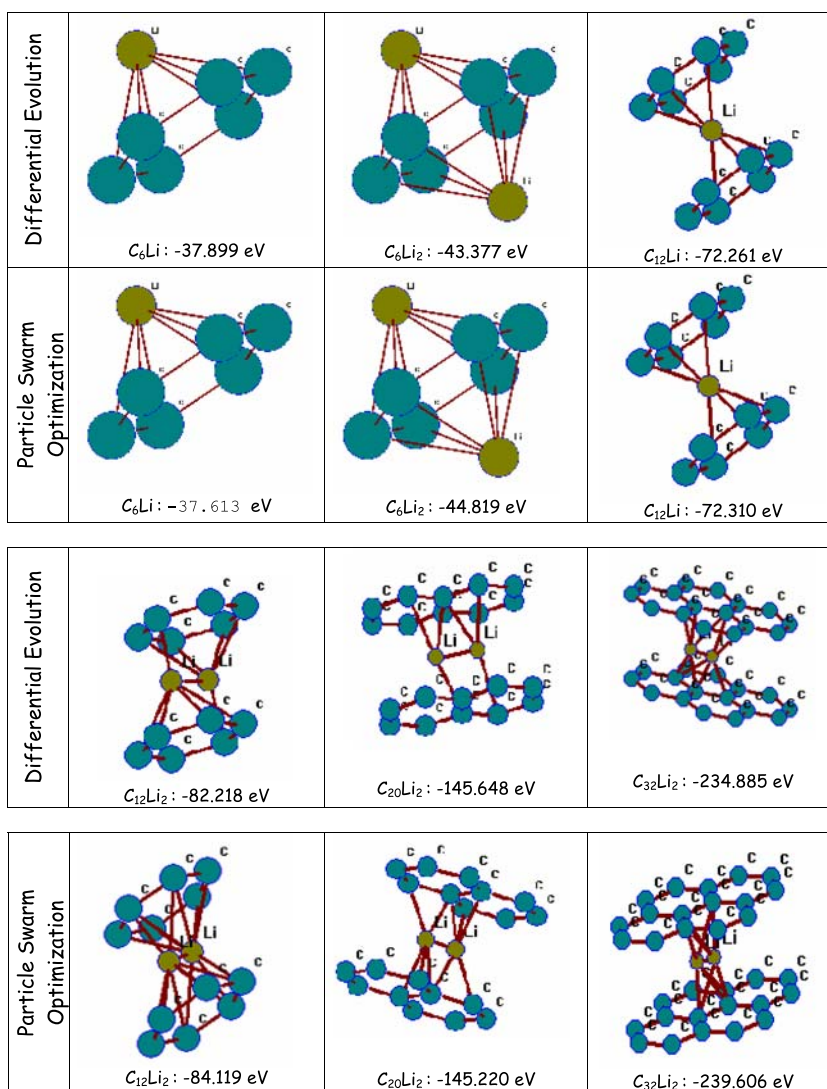


**Fig. 4** Optimized ground state configuration of various C-Li<sup>+</sup> assemblies computed using differential evolution and particle swarm optimization techniques.

arrangements were found to be different, and in most cases, the ground state energy values worked out to be significantly lower for the unconstrained assemblages, which happened primarily because the C-Li<sup>+</sup> attractive interaction worked out to be stronger than the Li<sup>+</sup>-Li<sup>+</sup> repulsion. Furthermore, as number of Li<sup>+</sup> increase in the system, number of C-Li<sup>+</sup> pair increases more than the Li<sup>+</sup>-Li<sup>+</sup> pair, which makes C-Li<sup>+</sup> interactions more dominant. Also, in case of the unconstrained problems, the evolutionary algorithms had more freedom, and they could easily and very efficiently weed out solutions with too closely spaced Li<sup>+</sup> ions, on the basis of their lower fitness values, ultimately locating configurations, which are energetically more favorable than what one would be able to obtain by imposing some external constraints. This difference in thermodynamic stability could be crucial for many battery applications, as a number of Li-C phases are known to be highly unstable, where this possibility of lowering the ground state energy would actually matter.

In most of the cases, particularly for the relatively complex configurations, the Particle Swarm calculations worked better than Differential Evolution leading to lower energy ground states at a lower number of function evaluation. At least in one case, the constrained  $C_{72}Li_8$  shown in Fig. 5, DE apparently failed to converge. The greedy approach that DE adopts by selecting only the stronger offspring, by pitting the child against its parent,<sup>[22,23]</sup> need not be effective in all situations. This very feature of DE that renders it into one of the fastest converging evolutionary algorithms, may also cause its occasional downfall, as encountered in the present case. Nonetheless, DE still remains a very strong contender for such calculations and in earlier studies it proved to be highly effective for the other cluster systems.<sup>[17-19]</sup> This impressive performance of PSO warrants further exploration of this emerging evolutionary technique, which very effectively retains the promising solutions, the so called *elites* in the genetic algorithms nomenclature, allows their propagation in the future generations and at

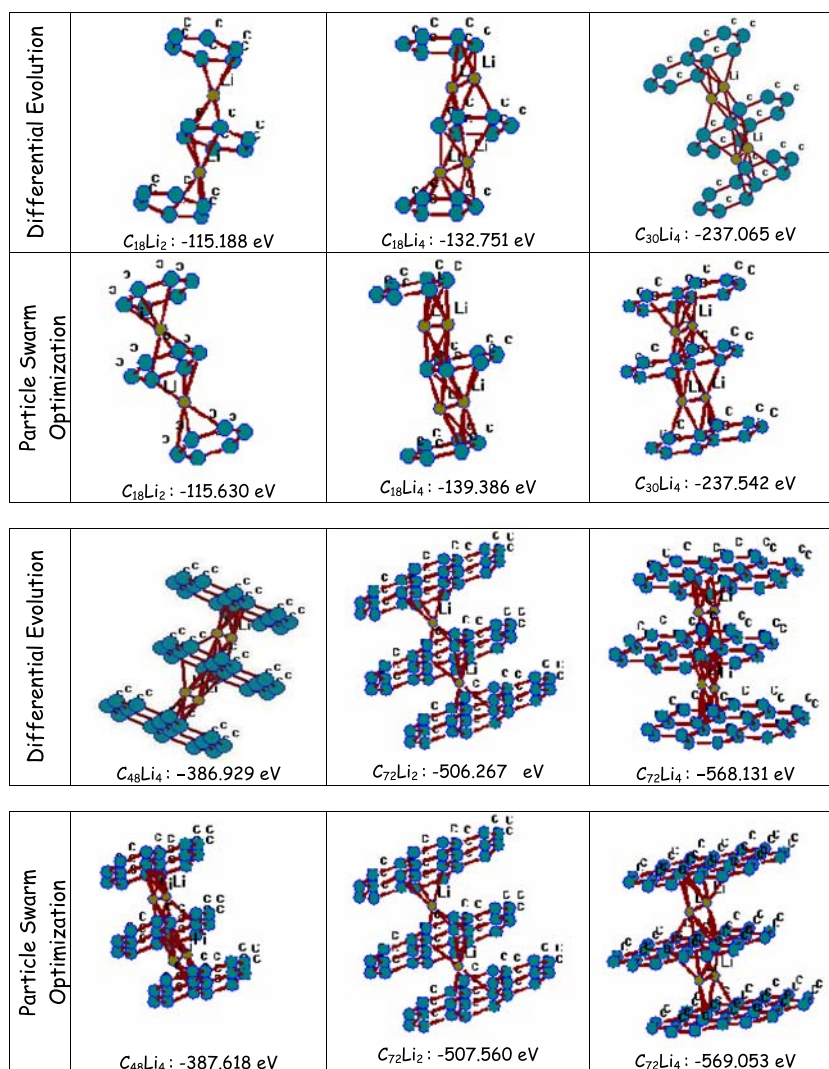


Fig. 4 Continued.

**Table 4 Constraints added for the locations of  $Li^+$** Invalid Location for  $Li^+$  $D_z < c, D_x < a, D_y < b$ Valid Location for  $Li^+$ 

All other cases

Remarks

 $a =$  > Distance between centers of adjacent hexagons in  $x$  direction $b =$  > Distance between centers of adjacent hexagons in  $y$  direction $c =$  > Inter-planar distanceThe distances between any two lithium ions in  $x$ ,  $y$  and  $z$  directions are  $D_x$ ,  $D_y$  and  $D_z$  respectively

the same time continuously improves and updates them. As stated before, when stripped of the allegory of flying birds, the PSO algorithm actually is a genetic algorithm where the elites participate very effectively in an elegantly crafted genetic *recombination*, without invoking a ruthless concern for the *fitness* maximization that has worked against DE in the present problem.

Both DE and PSO are however, global optimizers and their better performance compared to the ubiquitous MD techniques is actually not unexpected. Further adding to their advantages, these population-based approaches are also insensitive to the initial guess values, and therefore, it is really unnecessary for either DE or PSO to start with the same initial population, in order to converge to a particular final solution.

Our computed structures of  $C_6Li$ ,  $C_{12}Li_2$  and  $C_6Li_2$  emulate the basic symmetries of  $LiC_6$  and  $LiC_3$  reported elsewhere.<sup>[31]</sup> Experimental data on the Li-C assemblies are however, rather limited, the reason being the highly complicated processing routes for many of them. Synthesis of a lithium rich compound like  $LiC_2$ , for example, would require a pressure as high as 300 bars, and not to mention the heavy apparatus associated with it.<sup>[31]</sup> There are reports however, of the preparation of  $LiC_{12}$  and  $LiC_{18}$ .<sup>[31]</sup> The structures corresponding to both these stoichiometries have been revealed in this study through the calculations of  $C_{12}Li$ ,  $C_{48}Li_4$ ,  $C_{72}Li_6$  and  $C_{72}Li_4$  shown in Fig. 4 and 5.

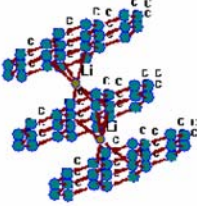
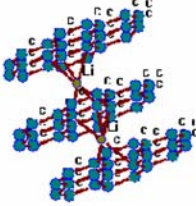
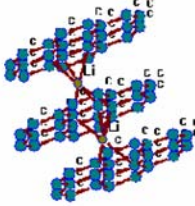
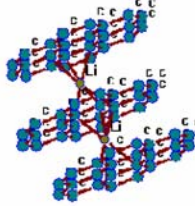
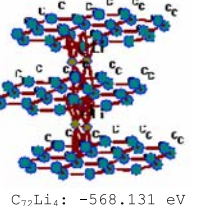
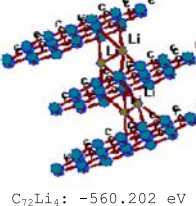
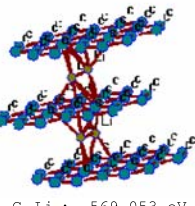
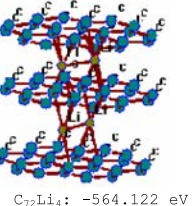
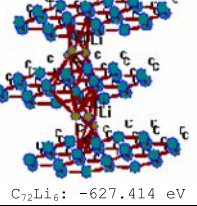
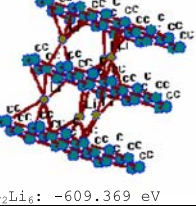
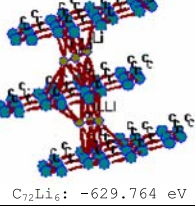
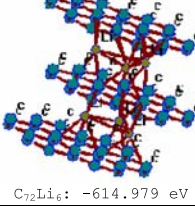
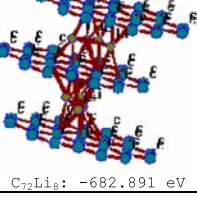
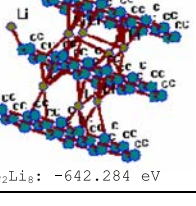
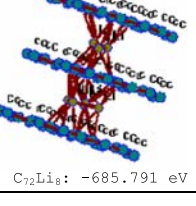
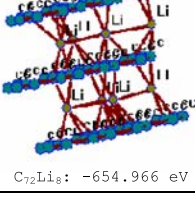
Differential Evolution		Particle Swarm Optimization	
Without constraints	With constraints	Without constraints	With constraints
 C <sub>72</sub> Li <sub>2</sub> : -506.267 eV	 C <sub>72</sub> Li <sub>2</sub> : -506.267 eV	 C <sub>72</sub> Li <sub>2</sub> : -507.582 eV	 C <sub>72</sub> Li <sub>2</sub> : -507.582 eV
 C <sub>72</sub> Li <sub>4</sub> : -568.131 eV	 C <sub>72</sub> Li <sub>4</sub> : -560.202 eV	 C <sub>72</sub> Li <sub>4</sub> : -569.053 eV	 C <sub>72</sub> Li <sub>4</sub> : -564.122 eV
 C <sub>72</sub> Li <sub>6</sub> : -627.414 eV	 C <sub>72</sub> Li <sub>6</sub> : -609.369 eV	 C <sub>72</sub> Li <sub>6</sub> : -629.764 eV	 C <sub>72</sub> Li <sub>6</sub> : -614.979 eV
 C <sub>72</sub> Li <sub>8</sub> : -682.891 eV	 C <sub>72</sub> Li <sub>8</sub> : -642.284 eV	 C <sub>72</sub> Li <sub>8</sub> : -685.791 eV	 C <sub>72</sub> Li <sub>8</sub> : -654.966 eV

Fig. 5 Constrained vs. unconstrained clusters.

The present study indicates the possibility of various alternate structures having the same stoichiometry as LiC<sub>12</sub> and LiC<sub>18</sub>, which the earlier experimental studies<sup>[31]</sup> could not resolve. In fact, despite immense practical interest that exists for the graphite intercalation compounds, reliable structural data, till date, are very limited for most of them. The present study is expected to fill some of the information gap in this area, and the alternate structures with same ground state stoichiometry opens up some more possibilities in the battery research albeit the fact that the nature of Li<sup>+</sup> diffusion in the graphite lattice is still not completely understood, and synthesizing some of the structures shown here would actually involve some very long term arduous work.

## 6. Concluding Remarks

The anodes in the lithium ion batteries currently rely heavily upon the Li<sup>+</sup>-C intercalation compounds formed within the framework of graphene sheets. Evolutionary Algorithms can efficiently resolve the phase configurations in such systems, as

demonstrated in this work. The possibility of pushing in Li<sup>+</sup> within carbon nanotubes would be an alternate possibility where some work has already begun.<sup>[32]</sup> In a follow-up step of this work we looked into that problem very rigorously, using once again, Genetic Algorithms of diverse kind.<sup>[33]</sup>

Here it is worth to mention that the PEF used in the present study represents C-Li<sup>+</sup> system reasonably well. The carbon portion of the PEF was well tested before to simulate various carbon nanosystems successfully.<sup>[34]</sup> The C-Li<sup>+</sup> and Li<sup>+</sup>-Li<sup>+</sup> pair interactions were specifically developed for the present study. The C-Li<sup>+</sup> interaction potential is generated from quantum chemical calculations and can be used for any C-Li<sup>+</sup> system without changing the parameters. However, the Li<sup>+</sup>-Li<sup>+</sup> interaction potential parameters can be changed and readjusted depending on the system considered. We have kept these parameters fixed for all the models considered in the present work.

The nominal differences that remained between MD and the evolutionary results shown in Fig. 2 and 3 could be attributed to various factors. In case of LiC<sub>6</sub>, the best performance of the MD calculations remained slightly inferior compared to those obtained through DE and PSO. For this configuration the converged result for MD at its best (-37.144 eV) is probably a



## Section I: Basic and Applied Research

local minimum at the near optimal range, of which it was unable to come out owing to the low temperature used in these calculations, a choice, as stated before, motivated by the fact that the neither DE nor PSO would consider any temperature effects, and our aim was to compare their efficacy at a comparable situation. Also, it needs to be emphasized that it really makes no difference for the DE and PSO that some of the assemblies, particularly the ones shown in Fig. 2, are actually quite simple, since searches for a global minimum were conducted in all cases assuming that the atoms could be anywhere in a three dimensional Cartesian space, the very same way as it would be done for the most complicated structures. Also, being totally derivative less, the evolutionary methods actually do not have a fixed stopping criteria. Here we made them to stop only after a prescribed number of generations. The MD calculations shown in the same figure were actually started with the evolutionary results in hand and the converged results appeared better than the similar calculations performed with not so specific starting values. This however, does not matter, as far as the efficiency of the evolutionary techniques go. Their global searching power is even better realized for more complicated cases, which the rest of the assemblies reported in this paper are all about, and many of those would be extremely difficult to resolve with the MD procedure. We did not report any more comparisons in this article, but for the nanotube cases MD technique inevitably produced inferior results than both DE and PSO, failing albeit for the larger and complicated assemblies.<sup>[33]</sup> That happened simply because of the relative lack of hill climbing ability of the MD technique that we have employed here. Some earlier *ab initio* studies conducted for the lithium ions in carbon nanotubes, found the energy contours to be highly multi-modal.<sup>[35]</sup> In fact it was reported<sup>[35]</sup> that several minima are located approximately at 2.2 Å from the wall, and their number increases with the increasing tube diameter. It is interesting to report that for the simple configuration presented in Fig. 2, the MD simulations could locate two stable local minima, each at a different height, and only the lower valued minimum is presented in Fig. 2. The other stable configuration in this case is at an energy value of -33.405 eV. Therefore, multi-modality of the energy contours does exist even when the lithium ions are inside the graphene sheets. For the simple case demonstrated in Fig. 2, the MD technique could overcome such local energy barriers, particularly with the excellent starting values provided by the evolutionary methods. For the larger systems it becomes increasingly difficult, however even then the evolutionary techniques continue to provide, even by a highly conservative estimate, at least some excellent near-optimality. Nonetheless, being stochastic, the evolutionary methods may not produce the best results in each and every case, even for the same problem different results might be obtained after the same number of function evaluations. Precisely for this reason it is advantageous to employ more than one algorithm, as it has been done there, since in an evolutionary paradigm each and every run may not be successful, not because of any particular demerit of the algorithm, but simply for randomly picking up some wrong pathway. However, if one algorithm fails the chances are that the other might work. It is therefore not surprising that in some cases DE performed a little better than PSO, although in most trials, the performance of PSO was superior. Finally, for the

Tersoff potential used in this study, although one can perhaps think about a more accurate representation of the energy functional, however, the efficacy of the Tersoff potential is being increasingly acknowledged and recognized in the pertinent engineering literature.<sup>[36]</sup>

## Acknowledgments

We owe a lot to Professor Bruce Harmon for his enthusiastic critique of the technical contents of this article, and the numerous suggestions that he provided to improve it with an enormous patience. We would also like to thank the two anonymous reviewers who read this article quite carefully and suggested some excellent revisions.

## References

1. J. Tersoff, New Empirical Approach for the Structure and Energy of Covalent Systems, *Phys. Rev. B*, 1988, **37**, p 6991–7000
2. J. Tersoff, Empirical Interatomic Potential for Carbon, with Applications to Amorphous Carbon, *Phys. Rev. Lett.*, 1988, **61**, p 2879–2882
3. W. Kohn and L.J. Sham, Self-consistent Equations Including Exchange and Correlation Effects, *Phys. Rev. A*, 1965, **140**, p A1133–A1138
4. A.D. Becke, Density-functional Thermochemistry. III. The Role of Exact Exchange, *J. Chem. Phys.*, 1993, **98**, p 5648–5652
5. C. Lee, W. Yang, and R.G. Parr, Development of the Colle-Salvetti Correlation-energy Formula into a Functional of the Electron Density, *Phys. Rev. B*, 1993, **37**, p 785–789
6. R. Krishnan, J.S. Kinkley, R. Seeger, and J.A. Pople, Self-consistent Molecular Orbital Methods. XX. A Basis Set for Correlated Wave Functions, *J. Chem. Phys.*, 1980, **72**, p 650–654
7. Gaussian-98 Rev. A.7 package. Gaussian Inc., 1998, Pittsburgh, PA 15106, USA
8. Z. Michalewicz, *Genetic Algorithms + Data Structures = Evolution Programs*. Springer, Berlin, 1999
9. M. Mitchell, *An Introduction to Genetic Algorithms*. Prentice-Hall, New Delhi, India, 1998
10. I.N. Egorov-Yegorov and G.S. Dulikravich, Chemical Composition Design of Superalloys for Maximum Stress, Temperature, and Time-to-rupture Using Self-adapting Response Surface Optimization, *Mater. Manuf. Processes*, 2005, **20**, p 569–590
11. N. Chakraborti, Genetic Algorithms in Materials Design and Processing, *Int. Mater. Rev.*, 2004, **49**, p 246–260
12. C.Z. Wang and K. M Ho, Material Simulations with Tight-binding Molecular Dynamics, *J. Phase Equilibria*, 1997, **18**, p 516–529
13. B. Hartke, Global Geometry Optimization of Clusters Using Genetic Algorithms, *J. Phys. Chem.*, 1993, **97**, p 9973
14. M. Iwamatsu, Global Geometry Optimization of Silicon Clusters Using the Space-fixed Genetic Algorithm, *J. Chem. Phys.*, 2000, **112**, p 10976
15. G. Klimeck, R.C. Bowen, T.B. Boykin, C. Salazar-Lazaro, T.A. Cwik, and A. Stoica, Si Tight-binding Parameters from Genetic Algorithm Fitting, *Superlattices Microstruct.*, 2000, **27**, p 77–88
16. J.A. Niesse and H.R. Mayne, Global Geometry Optimization of Atomic Clusters Using a Modified Genetic Algorithm in Space-fixed Coordinates, *J. Chem. Phys.*, 1996, **105**, p 4700–4706
17. N. Chakraborti, P. Mishra, and Ş. Erkoç, A Study of the Cu Clusters Using Gray-coded Genetic Algorithms and Differential Evolution, *J. Phase Equilibria Diffusion*, 2004, **25**, p 16–21
18. N. Chakraborti and R. Kumar, Re-evaluation of Some Select Si<sub>n</sub>H<sub>2m</sub> Clusters Using Genetic Algorithms, *J. Phase Equilibria*, 2003, **24**, p 132–139
19. N. Chakraborti, K. Misra, P. Bhatt, N. Barman, and R. Prasad, Tight-binding Calculations of Si-H Clusters Using Genetic Algorithms and

- Related Techniques: Studies Using Differential Evolution, *J. Phase Equilibria*, 2001, **22**, p 525–530
20. N. Chakraborti, P.S. De, and R. Prasad, Genetic Algorithms Based Structure Calculations for Hydrogenated Silicon Clusters, *Mater. Lett.*, 2002, **55**, p 20–26
  21. Ş. Erkoç, K. Leblebicioğlu, and U. Halici, Application of Genetic Algorithms to Geometry Optimization of Microclusters: A Comparative Study of Empirical Potential Energy Functions for Silicon, *Mater. Manuf. Process.*, 2003, **18**, p 329–339
  22. K. Price and R. Storn, Differential Evolution, *Dr Dobbs J.*, 1997, **22**, p 18+
  23. K.V. Price, R.M. Storn, and J.A. Lampinen, *Differential Evolution – A Practical Approach to Global Optimization*. Springer, Berlin, 2005
  24. N. Chakraborti and A. Kumar, The Optimal Scheduling of a Reversing Strip Mill: Studies Using Multipopulation Genetic Algorithms and Differential Evolution, *Mater. Manuf. Processes*, 2003, **18**, p 433–445
  25. T.D. Rane, R. Dewri, S. Ghosh, K. Mitra, and N. Chakraborti, Modeling the Recrystallization Process Using Inverse Cellular Automata and Genetic Algorithms: Studies Using Differential Evolution, *J. Phase Equilibria Diffusion*, 2005, **26**, p 311–321
  26. J.F. Kennedy, R.C. Eberhart, and Y. Shi, *Swarm Intelligence*. Morgan Kaufmann Pub, San Francisco, 2001
  27. S.P. Ghoshal, Optimizations of PID Gains by Particle Swarm Optimizations in Fuzzy Based Automatic Generation Control, *Electric Power Syst. Res.*, 2004, **72**, p 203–212
  28. S. He, Q.H. Wu, J.Y. Wen, J.R. Saunders, and R.C. Paton, A Particle Swarm Optimizer with Passive Congregation, *Biosystems*, 2004, **78**, p 135–147
  29. D.W. Heerman, *Computer Simulation Methods in Theoretical Physics*. Springer-Verlag, Berlin, Heidelberg, 1986
  30. S. Basu, Early Studies on Anodic Properties of Lithium Intercalated Graphite, *J. Power Sources*, 1999, **81**, p 200–206
  31. R. Janot and D. Guerard, Ball-milling in Liquid Media – Applications to the Preparation of Anodic Materials for Lithium-ion Batteries, *Prog. Mater. Sci.*, 2005, **50**, p 1–92
  32. A. Udomvech, T. Kerdcharoen, and T. Osotchan, First Principles Study of Li and Li<sup>+</sup> Adsorbed on Carbon Nanotube: Variation of Tubule Diameter and Length, *Chem. Phys. Lett.*, 2005, **406**, p 161–166
  33. N. Chakraborti, S. Das, R. Jayakanth, R. Pekoz, and Ş. Erkoç, Genetic Algorithms Applied to Li<sup>+</sup> Ions Contained in Carbon Nanotubes: An Investigation Using Particle Swarm Optimization and Differential Evolution along with Molecular Dynamics. *Mater. Manuf. Process.*, 2007, **22**, in press
  34. Ş. Erkoç, Stability of Carbon Nanostructures: Balls, Tubes, Rods, Toroids. In: N. Chakraborti and U.K. Chatterjee (Eds), Proceedings of the International Conference on Advances in Materials and Materials Processing (ICAMMP-2002). 1–3 February, 2002, IIT-Kharagpur, India. Tata McGraw-Hill Pub. Com. Ltd., New Delhi, 2002, pp. 356–363
  35. C. Garau, A. Frontera, D. Quiñero, A. Costa, P. Ballester, and P.M. Deyà, Ab Initio Investigations of Lithium Diffusion in Single-walled Carbon Nanotubes, *Chem. Phys.*, 2004, **297**, p 85–91
  36. Z.G. Huang, Z.N. Guo, X. Chen, T.M. Yue, S. To, and W.B. Lee, Molecular Dynamics Simulation for Ultrafine Machining, *Mater. Manuf. Process.*, 2006, **21**, p 393–397